

Received April 30, 2020, accepted May 26, 2020, date of publication June 15, 2020, date of current version June 26, 2020.

Digital Object Identifier 10.1109/ACCESS.2020.3002267

# Fabrication, Characterization and Simulation of Sputtered Pt/In-Ga-Zn-O Schottky Diodes for Low-Frequency Half-Wave Rectifier Circuits

VERONIKA ULIANOVA<sup>1</sup>, FARHAN RASHEED<sup>2</sup>,  
SAMI BOLAT<sup>1</sup>, (Graduate Student Member, IEEE), GALO TORRES SEVILLA<sup>1</sup>,  
YURI DIDENKO<sup>3</sup>, XIAOWEI FENG<sup>4</sup>, IVAN SHORUBALKO<sup>5</sup>, DOMINIK BACHMANN<sup>5</sup>,  
DMYTRO TATARCHUK<sup>3</sup>, MEHDI B. TAHOORI<sup>2</sup>, (Senior Member, IEEE),  
JASMIN AGHASSI-HAGMANN<sup>4</sup>, (Member, IEEE), AND YAROSLAV E. ROMANYUK<sup>1</sup>

<sup>1</sup>Laboratory for Thin Films and Photovoltaics, Empa–Swiss Federal Laboratories for Materials Science and Technology, 8600 Dübendorf, Switzerland

<sup>2</sup>Chair of Dependable Nano Computing, Karlsruhe Institute of Technology, 76131 Karlsruhe, Germany

<sup>3</sup>Department of Microelectronics, National Technical University of Ukraine “Igor Sikorsky Kyiv Polytechnic Institute”, 03056 Kyiv, Ukraine

<sup>4</sup>Institute of Nanotechnology, Karlsruhe Institute of Technology, 76344 Karlsruhe, Germany

<sup>5</sup>Transport at Nanoscale Interfaces Laboratory, Empa–Swiss Federal Laboratories for Materials Science and Technology, 8600 Dübendorf, Switzerland

Corresponding author: Veronika Ulianova (veronika.ulianova@empa.ch)

The EMPAPOSTDOCS-II programme was received funding from the European Union’s Horizon 2020 research and innovation programme under the Marie Skłodowska-Curie-Curie grant agreement number 754364. This study was also supported by the University of Geneva in the framework of Seed Funding, through the Swiss State Secretariat for Education, Research and Innovation (SERI), under Grant SFG 602.

**ABSTRACT** Amorphous In-Ga-Zn-O (IGZO) is a high-mobility semiconductor employed in modern thin-film transistors for displays and it is considered as a promising material for Schottky diode-based rectifiers. Properties of the electronic components based on IGZO strongly depend on the manufacturing parameters such as the oxygen partial pressure during IGZO sputtering and post-deposition thermal annealing. In this study, we investigate the combined effect of sputtering conditions of amorphous IGZO (In:Ga:Zn=1:1:1) and post-deposition thermal annealing on the properties of vertical thin-film Pt-IGZO-Cu Schottky diodes, and evaluated the applicability of the fabricated Schottky diodes for low-frequency half-wave rectifier circuits. The change of the oxygen content in the gas mixture from 1.64% to 6.25%, and post-deposition annealing is shown to increase the current rectification ratio from  $10^5$  to  $10^7$  at  $\pm 1$  V, Schottky barrier height from 0.64 eV to 0.75 eV, and the ideality factor from 1.11 to 1.39. Half-wave rectifier circuits based on the fabricated Schottky diodes were simulated using parameters extracted from measured current-voltage and capacitance-voltage characteristics. The half-wave rectifier circuits were realized at 100 kHz and 300 kHz on as-fabricated Schottky diodes with active area of  $200 \mu\text{m} \times 200 \mu\text{m}$ , which is relevant for the near-field communication (125 kHz – 134 kHz), and provided the output voltage amplitude of 0.87 V for 2 V supply voltage. The simulation results matched with the measurement data, verifying the model accuracy for circuit level simulation.

**INDEX TERMS** Amorphous In-Ga-Zn-O, capacitance-voltage characteristics, current-voltage characteristics, half-wave rectifiers, Schottky diodes, sputtering.

## I. INTRODUCTION

Amorphous indium-gallium-zinc oxide (In-Ga-Zn-O or IGZO) is an established material of electronic devices due to its optical transparency, high electron mobility, low temperature processability, mechanical flexibility and ease of

The associate editor coordinating the review of this manuscript and approving it for publication was Jenny Mahoney.

structuring because of the amorphous nature [1]. IGZO with Hall effect mobility of  $10 \text{ cm}^2\text{V}^{-1}\text{s}^{-1}$ , which is an order of magnitude higher than for hydrogenated amorphous silicon, is employed as the active channel in transparent thin-film transistors (TFTs) [2]. Nowadays, IGZO TFTs have been widely utilized in various applications such as active-matrix back planes of flexible organic light emitting diode displays in smart phones and tablet computers [3], [4].

Schottky diodes based on amorphous IGZO have been demonstrated for ultra-high frequency energy harvesters [5], memory devices [6], metal-semiconductor field-effect transistors [7], glucose sensors [8], and temperature sensors [9].

Schottky diodes based on amorphous oxide semiconductors often suffer from surfaces sensitivity to ambient exposure, which changes the concentration of intrinsic oxygen vacancies and induced trap states at the interfaces. For amorphous oxide semiconductors all manufacturing parameters such as pressure, temperature, atmosphere, elemental ratio, pre- and post-deposition treatments as well as a contact metal lead to the modification of oxygen concentration in the film itself and at the device interfaces, thus determining electrical properties of the final device. Most process parameters depend on the sputtering system configuration and need to be optimized for each individual case. Additionally, pre- or post-deposition treatments are selected according to the properties of the materials and interfaces.

UV-ozone treatment [10] or oxygen plasma treatment [11] of Pd bottom electrode have been demonstrated for reducing the IGZO subgap states and Fermi level pinning. Introducing of 20% O<sub>2</sub> during the sputtering of IGZO after bottom electrode treatment and post-annealing at 200°C were applied to fabricate Schottky diodes with a rectification ratio up to 10<sup>8</sup> and ideality factor of 1.22 [11]. Thermal annealing at 200°C and an oxygen-containing atmosphere were utilized for the fabrication of the AgO<sub>x</sub>/IGZO Schottky diodes with rectification ratio of 10<sup>9</sup> at ±2V and an ideality factor of 1.7 [12]. The Pt/IGZO Schottky diodes on flexible plastic substrates operating beyond 2.45 GHz were fabricated by applying UV-ozone treatment and 3% O<sub>2</sub> atmosphere during the IGZO sputtering without any thermal annealing process [13]. Gradual doping of oxygen from 0% to 37.5% along the vertical profile of the a-IGZO layer allowed achieving the transparent conducting oxide/a-IGZO Schottky junction with rectification ratio of 10<sup>3</sup> [14].

It has been reported that the inclusion of oxygen during the noble metal deposition can reduce the oxygen deficiency at the Pt-IGZO Schottky interface, resulting in a barrier height of 0.92eV and an ideality factor of 1.36 [15].

Previous studies report different O<sub>2</sub> levels, annealing temperatures, annealing time and additional treatment of metal contact for obtaining best performance of Schottky diodes in terms of ideality factor, rectification ratio, Schottky barrier height, and cut-off frequency (Table 1), and focus on high-frequency and ultra-high frequency applications. The flow chart for the proposed systematic study on a-IGZO Schottky diodes development and testing is presented in Fig. 1. We performed the fabrication and current-voltage (*I-V*) and capacitance-voltage (*C-V*) characterization of the vertical thin-film Pt-IGZO-Cu Schottky diodes. The process optimization was proposed based on the analysis of the combined effect of the oxygen-containing atmosphere for sputtering of a-IGZO (In:Ga:Zn=1:1:1) and post-deposition thermal annealing on the characteristics of the fabricated diodes. Transient simulation of a low-frequency half-wave

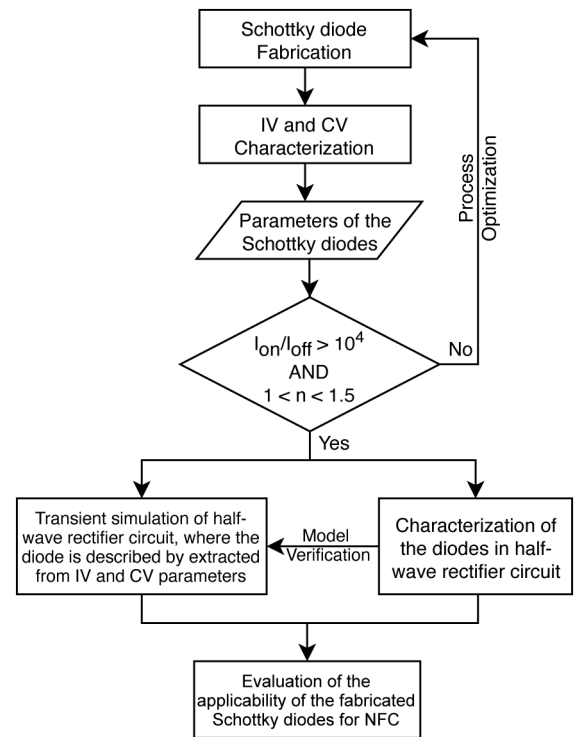


**FIGURE 1.** Flow chart for the a-IGZO Schottky diode development and testing in the half-wave rectifier circuit.

rectifier circuit, where the Schottky diodes were described by extracted from *I-V* and *C-V* parameters, and characterization of the fabricated diodes in the circuit were realized to evaluate the potential application of the Pt-IGZO Schottky diodes for the near-field communication (NFC) 125 kHz – 134 kHz.

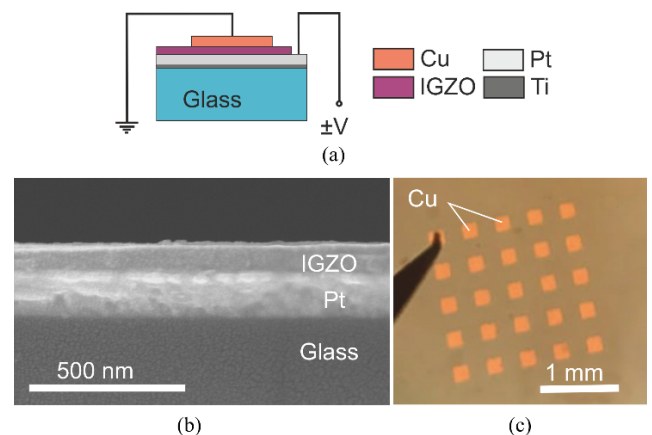


**FIGURE 2.** (a) Structure of the vertical Schottky diode Ti-Pt/IGZO/Cu, (b) SEM image of the a-IGZO Schottky diode, and (c) top-view microscope photograph of the array of the fabricated diodes on the substrate.

## II. FABRICATION

Vertical IGZO Schottky diodes (Fig. 2) were fabricated on alkali-free borosilicate glass (Corning 7059) to prevent a contamination of IGZO semiconductor film with alkali metals

**TABLE 1. Characteristics of the Schottky diodes fabricated in different process parameters.**

Parameter Contact metal	Contact area, $\mu\text{m}^2$	O <sub>2</sub> during IGZO sputtering	Treatment before IGZO sputtering	$T_{ann}$ , °C	$t$ , h	$n$	$I_{on}/I_{off}$	$\phi_b$ , eV	$R_s$ , Ohm	$V_{bi}$ , V	$N_{depl}$ , $\text{cm}^{-3}$	Cut-off frequency	Ref.
Pd	$10^4$	20%	UV-ozone	150	1	1.51	$10^7$	0.79	64.9	0.65	$1.4 \times 10^{17}$	–	10
Pd	$10^4$	20%	UV-ozone	150	2	1.71	$10^6$	0.72	23.6	0.75	$6 \times 10^{17}$	–	10
Pd	$1.2 \times 10^4$	20%	O <sub>2</sub> plasma	200	*	1.22	$10^8$	0.85	160	0.33	$7.9 \times 10^{15}$	1.8 GHz	11
Pd	200	20%	O <sub>2</sub> plasma	200	*	1.24	$10^8$	0.83	226	0.38	$1.4 \times 10^{17}$	1.1 GHz	11
AgO <sub>x</sub>	$1.28 \times 10^4$	–	–	150	1	1.71	$10^9$	1.14	694	0.94	$9.8 \times 10^{17}$	–	12
Pt	200	3%	–	–	–	2.1	$10^3$	0.51	$10^4$	0.45	–	6.3 GHz	13
Pt	$3 \times 10^4$	–	–	–	–	1.36	$10^6$	0.92	507	0.6	$4.1 \times 10^{18}$	6 MHz	15
Pt	$3 \times 10^4$	3%	–	–	–	1.56	$10^4$	0.72	138	0.46	$3.5 \times 10^{18}$	–	15
Pt	$9 \times 10^4$	6.9 Pa	–	200	1	1.04	$10^8$	1.2	300	0.38	$3.6 \times 10^{16}$	–	16
Pt	$4 \times 10^4$	6.25%	–	200	1	1.39	$10^7$	0.75	4.24	0.55	$7.7 \times 10^{17}$	–	this work

Where  $T_{ann}$  is annealing temperature,  $t$  is annealing time,  $n$  is ideality factor,  $\phi_b$  is Schottky barrier height,  $R_s$  is series resistance,  $V_{bi}$  is built-in potential,  $N_{depl}$  is charge density at depletion region, \*no value is specified

and minimize defects formation on the metal-semiconductor interface. First, the substrate was cleaned in a diluted acetic acid solution and then deionized water in an ultrasonic bath at 80°C for 40 min. Since electron affinity of IGZO with an atomic ratio of In:Ga:Zn=1:1:1 equals to 4.16 eV [17], metals with work function exceeding 5 eV are required to achieve a high potential barrier. The Pt thin film was deposited by radio frequency (RF) sputtering on a Ti adhesive layer on the glass substrate at a pressure of 0.28 Pa and a power density of  $2.96 \text{ W} \cdot \text{cm}^{-2}$  to form the Schottky contact. Total thickness of the bottom electrode was about 100 nm.

Continuous amorphous IGZO thin films (60-70 nm) were deposited by RF magnetron sputtering at room temperature from an IGZO ceramic target (composition In:Ga:Zn = 1:1:1) in an Ar/O<sub>2</sub> atmosphere with oxygen concentrations of 1.64%, 2.44% or 6.25% at a working pressure of 0.6 Pa and a power density of  $1 \text{ W} \cdot \text{cm}^{-2}$ . Before the deposition of the top contact, the samples were annealed at 200°C for 1 hour on a hot plate in air. Similar post-deposition annealing process was applied to enhance the electrical performance of IGZO diodes [10], [16], [18].

As the final step, ohmic Cu top contact was evaporated through a metal mask under high vacuum ( $< 4 \cdot 10^{-4} \text{ Pa}$ ). The area of the contact was  $200 \mu\text{m} \times 200 \mu\text{m}$  and the thickness of the layer was about 70 nm (Fig. 2 (c)).

Current-voltage and capacitance-voltage characteristics of the diodes were measured in air at room temperature in dark using Keithley 4200 characterization system; electrodes were contacted using a probe station Karl Suss PM8. The function generator (3022B Tektronix with 50 Ohm output) and oscilloscope (Wavesurfer 3034) were used for the diodes characterization in the half-wave rectifier circuit.

### III. CHARACTERIZATION AND SIMULATION

#### A. CURRENT-VOLTAGE CHARACTERIZATION

The typical current density – voltage characteristics of the Schottky diodes fabricated at 1.64%, 2.44%, and 6.25% of oxygen during IGZO RF sputtering and after thermal

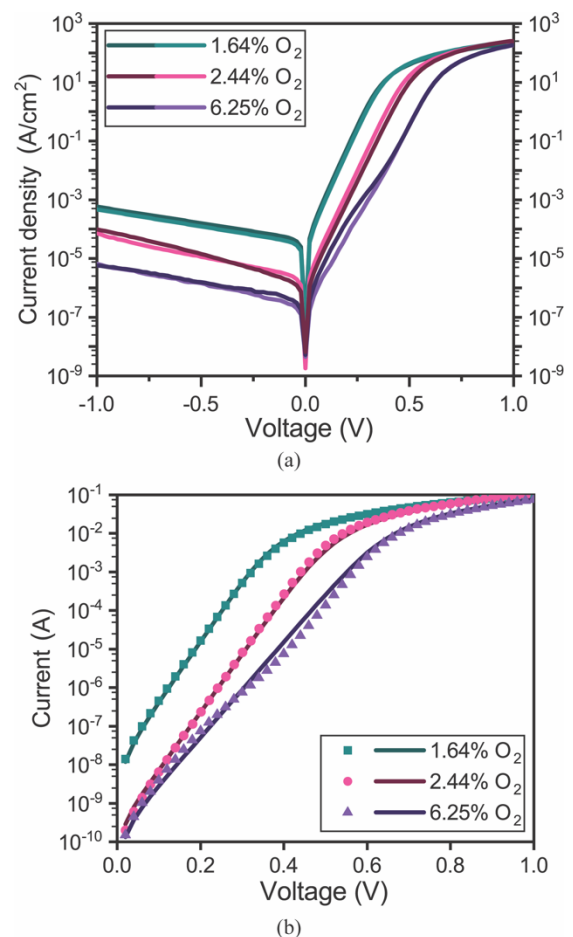


**FIGURE 3. Current-voltage characteristics of the devices fabricated at variable oxygen content of the Ar/O<sub>2</sub> gases during a-IGZO RF sputtering: (a) experimental characteristics for two different devices on the substrate at the same oxygen content are presented by color gradient and (b) current-voltage forward characteristics of Pt-IGZO-Cu Schottky diodes (symbols represent experimental values, and full lines represent fitted).**

annealing are presented in Fig. 3, where color gradients correspond to the experimental characteristics for two different devices on the substrate at the same oxygen content.

The standard deviation of current density for two different devices fabricated at the same oxygen content is less than 0.5% for all analyzed groups of samples. The effect of annealing on the rectification ratio ( $I_{on}/I_{off}$ ) depends on the initial oxygen content during the IGZO sputtering [18]. The maximum current density of 250 A/cm<sup>2</sup> at 1 V is observed for the samples deposited at lower oxygen content after thermal annealing. This effect can be explained by the increase of the free charge density when lowering oxygen concentration during thermal annealing.

The improvement of the off-current, and thus rectification ratio up to 10<sup>7</sup> at ±1 V is observed for the samples fabricated at 6.25% of oxygen after annealing at 200°C due to the reduction of interfacial defects.

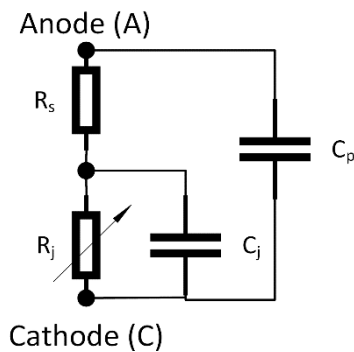


FIGURE 4. The equivalent circuit for the Schottky diode.

The equivalent circuit for the Schottky diode is shown in Fig. 4, where  $R_s$  represents the series resistance including the bulk resistance of the IGZO and the ohmic contact resistance. The junction resistance of the diode is denoted as  $R_j$ . The  $R_j$  is a voltage-dependent resistor that represents the diode itself. The capacitances  $C_j$  and  $C_p$  represent the junction capacitance (caused by the depletion layer) and the parasitic capacitance, respectively.

The current through a Schottky diode is described by the thermionic emission of majority carriers over the junction barrier [19]:

$$I = I_s \{ \exp[q(U - IR_s)/nkT] - 1 \}, \quad (1)$$

where  $I_s$  is the saturation current;  $q$  is the electron charge;  $n$  is the ideality factor;  $k$  is the Boltzmann constant; and  $T$  is the absolute temperature.

To extract the parameters of the Schottky diode, first a tangent line is built on the linear range of the forward current-voltage ( $I$ - $V$ ) characteristic using numerical methods to extract  $R_s$ ,  $R_s = dU/dI$ . The logarithm of the measurement data of the diode current is taken to approximate the experimental curve to a straight line. Then the linearized data set obtained by the least squares method is approximated using the first-degree polynomial. The initial equation (1) becomes:

$$\ln I = \ln I_s + \ln \{ \exp[q(U - IR_s)/nkT] - 1 \}, \quad (2)$$

and it can be viewed as a straight-line equation  $y = ax + b$ , where  $y = \ln I$ ,  $ax = \ln \{ \exp[q(U - IR_s)/nkT] - 1 \}$ ,  $b = \ln I_s$ . The saturation current is calculated after determination of the polynomial coefficients as  $I_s = \exp(b)$ .

On the other hand,  $I_s$  can be expressed [19]:

$$I_s = AA^*T^2 \cdot \exp(-q\phi_b/kT), \quad (3)$$

where  $A$  is the area of the diode;  $A^*$  is the effective Richardson constant which for IGZO has a theoretical value of 41 A·cm<sup>-2</sup>·K<sup>-2</sup> [20];  $\phi_b$  is the Schottky barrier height and it can be calculated as:

$$\phi_b = \ln \left( I_s / AA^*T^2 \right) kT / q. \quad (4)$$

Another approach to extract the barrier height is to employ density-functional theory (DFT) calculations, as [1]. However, because the oxygen concentration in our a-IGZO films is not precisely determined, we rely on the extraction of the barrier height using equation (4).

The barrier height for an n-type semiconductor is defined by:

$$\phi_b = W_{Pt} - \chi_{IGZO}, \quad (5)$$

where  $W_{Pt}$  is the work functions of the metal ( $W_{Pt} = 5.4$  eV [19]),  $\chi_{IGZO}$  is the electron affinity of the semiconductor and is calculated using equation (5).

After re-arranging terms in equation (1) the ideality factor  $n$  is calculated:

$$n = \frac{q(U - IR_s)}{kT \ln(I/I_s + 1)}. \quad (6)$$

The values of  $U$  and  $I$  are taken from the linear range of the forward current-voltage characteristic for calculation of the ideality factor  $n$ . Then the value of  $R_s$  is revised by solving of the equation (1) in relation to  $R_s$ , using calculated  $I_s$  and  $n$ , and experimental data of  $U$  and  $I$ . The method of successive approximations with a maximum relative error of 5% was used. The experimental and fitted current-voltage characteristics of fabricated diodes are presented in Fig. 3 (b).

## B. CAPACITANCE-VOLTAGE CHARACTERIZATION

Because the area of the fabricated Schottky diodes is large we focused on the low-frequency range, suitable for the NFC applications. Capacitance-voltage characteristics were measured in the range of test signal of 30 kHz – 1 MHz, where the lowest noise level of the capacitance was observed. Frequency shift in this range did not lead to a significant change of the measured capacitance and  $C$ - $V$  characteristics obtained at 100 kHz are shown in Fig. 5 (a). The capacitance increases slowly with decreasing reverse bias voltage, indicating that the width of the depletion region varied with the applied bias voltage. The area of the diodes limits the capacitance to the values of 100 pF, 110 pF and 170 pF at reverse bias (Fig. 5 (a)) for the samples fabricated at 1.64%, 2.44% and 6.25% of oxygen during IGZO RF sputtering, respectively. The increase of capacitance is caused by the combination of two effects: different free carrier density in IGZO layer after



the sputtering and post-deposition annealing in air. Elevated oxygen partial pressure reduces the concentration of oxygen vacancies, thus lowering the free electron concentration in the IGZO layer [21], but during thermal annealing in air the free charge density and the surface defect density increase as oxygen is leaving the film [10].

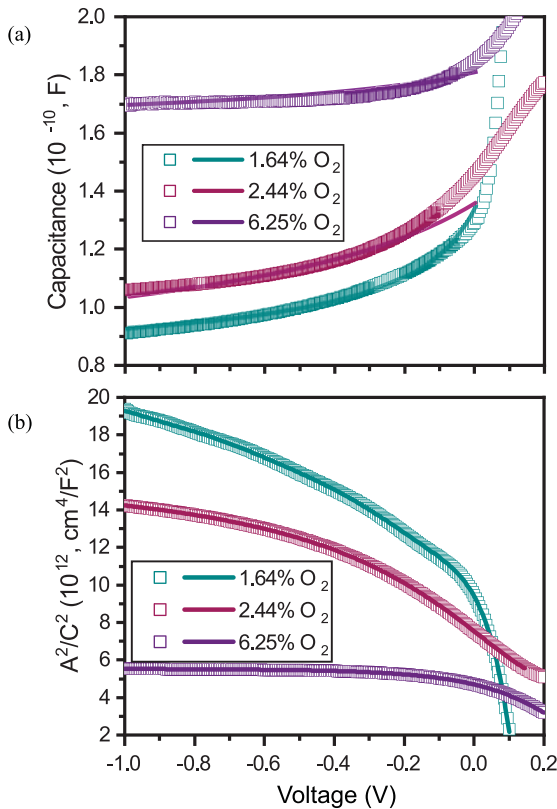


**FIGURE 5.** (a) Capacitance-voltage characteristics and (b)  $A^2/C^2$  plots of Pt-IGZO-Cu Schottky diodes fabricated at variable oxygen content of the Ar/O<sub>2</sub> gases during a-IGZO RF sputtering (symbols represent experimental values, and full lines represent simulation results).

To analyze experimental capacitance-voltage characteristics of the diodes, the  $(A/C)^2$  data set is approximated by the least squares method (Fig. 5 (b)). The capacitance of a Schottky junction is given by [5]:

$$\frac{A^2}{C^2} = \frac{2}{\epsilon_s \epsilon_0 N_{depl}} (V_{bi} - kT/q - U), \quad (7)$$

where  $\epsilon_s$  is the static dielectric constant of the semiconductor,  $\epsilon_0$  is the dielectric constant of vacuum,  $V_{bi}$  is the built-in potential, and  $N_{depl}$  is the charge density at depletion region.

The x-intercept of a tangent line to the linear range of  $(A/C)^2(U)$  corresponds to the value of the built-in potential  $V_{bi}$ . After re-writing equation (7) one obtains:

$$\frac{A^2}{C^2} = \frac{2}{\epsilon_s \epsilon_0 N_{depl}} \left( \frac{kT}{q} + U \right) + \frac{2V_{bi}}{\epsilon_s \epsilon_0 N_{depl}}. \quad (8)$$

A tangent line is described by  $y = Kx + M$ , whereby  $y = A^2/C^2$ ,  $K = -2/\epsilon_s \epsilon_0 N_{depl}$ ,  $x = kT/q + U$ , and  $M = 2V_{bi}/(\epsilon_s \epsilon_0 N_{depl})$ .

After solving the following system of equations:

$$\begin{cases} y_1 = Kx_1 + M, \\ y_2 = Kx_2 + M, \end{cases} \quad (9)$$

where  $x_1$  and  $y_1$  correspond to  $U_1$ , and  $x_2$  and  $y_2$  correspond to  $U_2$ , and if  $y = 0$ , one obtains  $U = (kT/q + M/K) = V_{bi}$ .

The dielectric constant of the semiconductor is calculated from  $C = \epsilon_s \epsilon_0 A/d$  assuming that diodes are depleted at  $-1$  V and  $d$  is the thickness of IGZO layer. The charge density at the depletion region is calculated as  $N_{depl1} = -2/K\epsilon_s \epsilon_0 q$  and  $N_{depl2} = 2V_{bi}/M\epsilon_s \epsilon_0 q$ . The mean value is taken to minimize the calculation error.

In order to extract junction capacitance  $C_j$  and parasitic capacitance  $C_p$ , the transient simulation for the Schottky diode is enabled by modeling the capacitance-voltage behavior of the Schottky diode. The total capacitance  $C_{tot}$  is given by equation (10) [22]:

$$C_{tot} = C_j \left( 1 - \frac{V}{V_{bi}} \right)^{-1/2} + C_p. \quad (10)$$

The junction capacitance  $C_j$  and parasitic capacitance  $C_p$  are extracted from the  $C$ - $V$  measurements of the devices in the reverse biased region. The Levenberg–Marquardt algorithm is used to estimate the  $C_p$  and  $C_j$  by reducing the fitting error between the measured and modeled  $C$ - $V$  curves. The model matches very well with the measurement data with a maximum relative error of 1.22% (Fig. 5 (a)).

**TABLE 2.** Characteristics of the Schottky diodes extracted from  $I$ - $V$  and  $C$ - $V$  measurements.

Parameters	O <sub>2</sub> , %	1.64	2.44	6.25
$I_{on}/I_{off}$		$10^5$	$10^6$	$10^7$
$I_s$ , A		$1.5 \times 10^{-8}$	$9.2 \times 10^{-10}$	$3.9 \times 10^{-10}$
$\phi_b$ , eV		$0.64 \pm 0.01$	$0.72 \pm 0.03$	$0.75 \pm 0.03$
$\chi_{IGZO}$ , eV		$4.76 \pm 0.01$	$4.68 \pm 0.03$	$4.65 \pm 0.03$
$n$		$1.11 \pm 0.02$	$1.18 \pm 0.07$	$1.39 \pm 0.09$
$R_s$ , Ohm		$5.94 \pm 0.32$	$4.14 \pm 0.03$	$4.24 \pm 0.16$
$V_{bi}$ , V		$0.15 \pm 0.03$	$0.37 \pm 0.01$	$0.55 \pm 0.03$
$\epsilon_{IGZO}$		$17.5 \pm 0.5$	$17.7 \pm 0.1$	$19.4 \pm 0.7$
$N_{depl}$ , cm <sup>-3</sup>		$1.06 \times 10^{17}$	$3.48 \times 10^{17}$	$7.69 \times 10^{17}$
$C_j$ , F		$6.4 \times 10^{-11}$	$7.8 \times 10^{-11}$	$5.7 \times 10^{-11}$
$C_p$ , F		$7.1 \times 10^{-11}$	$5.7 \times 10^{-11}$	$1.5 \times 10^{-10}$

Extracted electrical characteristics of the fabricated diodes are summarized in Table 2. It can be seen, that the increase of the oxygen content during IGZO RF sputtering from 1.64% to 6.25% and post-deposition thermal annealing enhances the rectification ratio, Schottky barrier height, ideality factor, built-in voltage, dielectric constant and charge density at the depletion region, but decreases electron affinity of IGZO and parasitic capacitance. Fig. 6 shows the schematic energy band diagram of Pt/IGZO Schottky contact with the obtained parameters. The maximum value of the junction capacitance  $C_j$  and minimum value of the series resistance  $R_s$  are obtained for the devices sputtered at 2.44% of oxygen.

It is difficult to directly compare the device parameters from the present study with the previously reported results

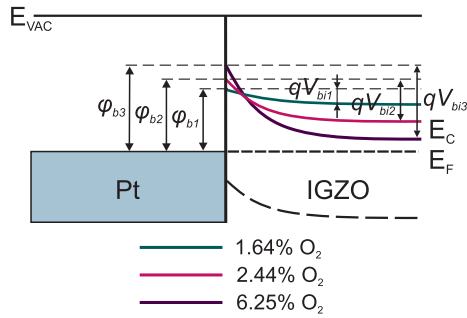


**FIGURE 6.** Schematic energy band diagram of Pt-IGZO Schottky contact fabricated at variable oxygen content of the Ar/O<sub>2</sub> gases during a-IGZO RF sputtering ( $V_{bi1}$  and  $\phi_{b1}$ ,  $V_{bi2}$  and  $\phi_{b2}$ ,  $V_{bi3}$  and  $\phi_{b3}$  correspond to 1.64%, 2.44% and 6.25% of oxygen, respectively).

because of the difference in the process parameters, size of the structures and contact metals. However, following observations can be made. Compared to the reported Pt-IGZO-ITO diodes based on IGZO films with a higher Ga composition and sputtered at 1%, 5% or 10% of oxygen [23], a significant improvement in rectification ratio to  $10^7$  of the Schottky diodes fabricated in this study (In:Ga:Zn=1:1:1) was achieved. It was demonstrated that thermal annealing at 200°C helped to improve the rectification ratio of Pt-IGZO Schottky diodes based on IGZO sputtered in 2.44% of O<sub>2</sub> by two orders of magnitude in comparison with the previously reported diodes based on IGZO sputtered in 3% of O<sub>2</sub> [13]. The higher values of the rectification ratio were obtained for the fabricated diodes without any oxygen or ozone plasma treatment of the bottom electrode compared to the reported Pd-IGZO-Mo structures [11], where bottom contact treatment prior to IGZO deposition was used. The improvement of the fabricated diode parameters can be explained by the optimization of the process parameters and combined effect of the controlled oxygen atmosphere during deposition and post-deposition thermal annealing, which modified the free charge and surface defect densities in the Pt-IGZO structure.

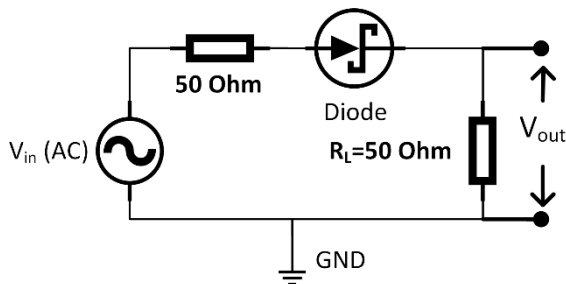


**FIGURE 7.** The half-wave rectifier circuit.

### C. HALF-WAVE RECTIFIER

To demonstrate the functionality of the fabricated diodes in circuit, we realized a half-wave rectifier and characterized its performance. Using the aforementioned models, we performed the transient simulation of the circuit and compared the results with the experiments. The half-wave rectifier circuit is shown in Fig. 7. A signal generator is used to

generate the sinusoidal input voltage  $V_{in}$  for the rectifier. The signal generator has an internal 50 Ohm resistance which is represented by resistor connected to the anode of the diode in the circuit. The diode is connected to the oscilloscope and the signal generator with probes. Probes have a resistance of 50 Ohm which represent the load resistor ( $R_L$ ) of the half-wave rectifier. Measurements were performed with an input voltage of  $\pm 2$  V and frequency of 100 kHz and 300 kHz and presented in Fig. 8. The frequency range was chosen based on the target application frequency i.e. near-field communication 125 kHz – 134 kHz [24]. The maximum output voltage is 0.77 V for 2 V supply voltage for the Schottky diodes fabricated at 1.64% O<sub>2</sub> because of the voltage drop across the input resistor and the diode, which is 0.77 V and 0.46 V, respectively (Fig. 8 (a, left)). The simulations were performed using open-source Ngspice simulator [25].

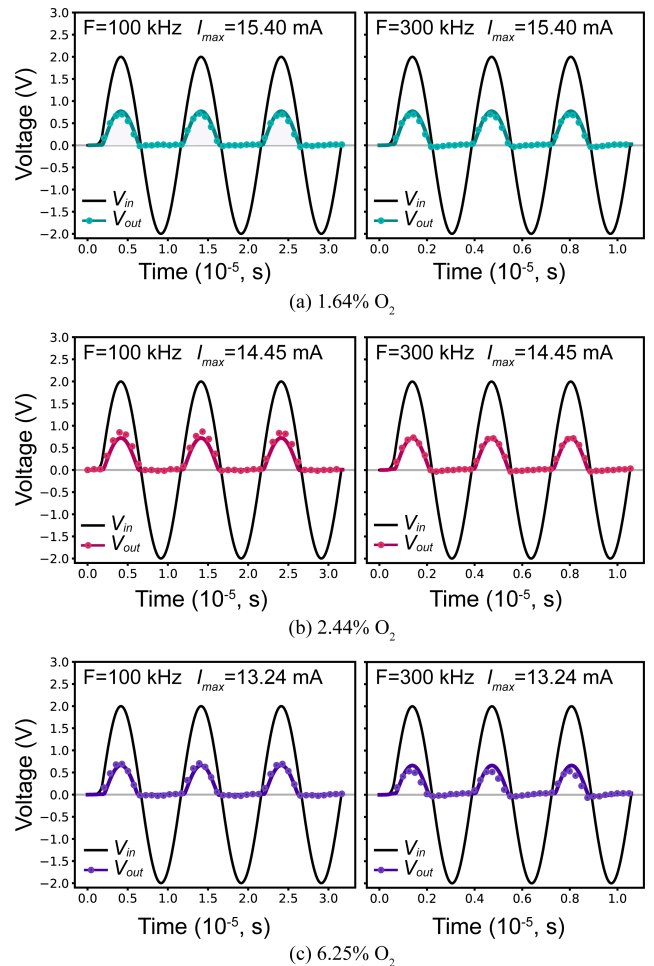


**FIGURE 8.** Half-wave rectifier input and output waveforms measured at 100 kHz and 300 kHz for Pt-IGZO-Cu Schottky diodes fabricated at variable oxygen content (dots represent experimental values, and full lines represent simulation results): (a) 1.64% O<sub>2</sub>, (b) 2.44% O<sub>2</sub>, and (c) 6.25% O<sub>2</sub>;  $V_{in}$  is the input voltage,  $V_{out}$  is the output voltage, and  $I_{max}$  is the peak current.

It can be seen in Fig. 8 that simulation results match with measurements. It is observed that the output voltage amplitude  $V_{out}$  decreases with the increase of the oxygen

pressure in the simulation because the barrier height ( $\varphi_b$ ) is increased and more potential is required to turn-on the diode compared to the diode with lower  $\varphi_b$ . In the measurement, it is also decreased except for the device fabricated at 2.44% O<sub>2</sub> where the output voltage of 0.87 V at 100 kHz is highest. This behavior cannot be explained and requires further investigation. It is observed that at 300 kHz the rectified output amplitude  $V_{out}$  decreases compared to the 100 kHz measurements. This effect is observed only for the devices that were fabricated at 2.44%, and 6.25% of oxygen content during IGZO RF sputtering. The reduction in the rectified output voltage amplitude can be attributed to the decreased barrier height at high frequencies, which is not captured by the presented model as the capacitance model does not include the frequency dependence. However, this effect has been reported before [26] and can be our future research task for the presented diodes.

#### IV. CONCLUSION

For the deposition of amorphous oxide semiconductors absolute values of the process parameters need to be optimized for each individual case depending on the target composition and sputtering system configuration. It was demonstrated that the concentration of oxygen in the Ar/O<sub>2</sub> mixture during IGZO RF sputtering and post-deposition thermal annealing affected the properties of the vertical thin-film Pt-IGZO-Cu Schottky diodes. The increase of the oxygen content during sputtering from 1.64% to 6.25% and post-deposition annealing at 200°C led to increasing the rectification ratio from 10<sup>5</sup> to 10<sup>7</sup> at ±1 V, Schottky barrier height from 0.64 eV to 0.75 eV, and ideality factor from 1.11 to 1.39.

The half-wave rectifier circuits based on the Schottky diodes were simulated using parameters extracted from the measured  $I$ - $V$  and  $C$ - $V$  characteristics and characterized at 100 kHz and 300 kHz, which is relevant for the near-field communication (125 kHz – 134 kHz). The Schottky diodes with active area of 200 μm × 200 μm fabricated at 1.64% O<sub>2</sub> provided the output voltage amplitude of 0.77 V for 2 V supply voltage at 100 kHz. However, the highest output voltage amplitude of 0.87 V was observed for the samples fabricated at 2.44% O<sub>2</sub> and slightly decreased for the Schottky diodes fabricated at higher oxygen pressure. The simulation results matched with the measurements, verifying the model accuracy for circuit level simulation.

#### ACKNOWLEDGMENT

The authors acknowledge access to the Scanning Probe Microscopy User Lab at Empa.

#### REFERENCES

- [1] T. Kamiya, K. Nomura, and H. Hosono, "Present status of amorphous In-Ga-Zn-O thin-film transistors," *Sci. Technol. Adv. Mater.*, vol. 11, no. 4, Feb. 2010, Art. no. 044305, doi: [10.1088/1468-6996/11/4/044305](https://doi.org/10.1088/1468-6996/11/4/044305).
- [2] K. Nomura, H. Ohta, A. Takagi, T. Kamiya, M. Hirano, and H. Hosono, "Room-temperature fabrication of transparent flexible thin-film transistors using amorphous oxide semiconductors," *Nature*, vol. 432, no. 7016, pp. 488–492, Nov. 2004, doi: [10.1038/nature03090](https://doi.org/10.1038/nature03090).
- [3] M. Nag, K. Obata, Y. Fukui, K. Myny, S. Schols, P. Vicca, T. H. Ke, S. Smout, M. Willeghems, M. Ameys, A. Bhoolakam, R. Müller, B. Cobb, A. Kumar, J.-L. van der Steen, T. Ellis, G. Gelinck, J. Genoe, P. Heremans, and S. Steudel, "20.1: Flexible AMOLED display and gate-driver with self-aligned IGZO TFT on plastic foil," in *SID Symp. Dig. Tech. Papers*, vol. 45, no. 1, Jun. 2014, pp. 248–251, doi: [10.1002/j.2168-0159.2014.tb00068.x](https://doi.org/10.1002/j.2168-0159.2014.tb00068.x).
- [4] S. K. Dargar and V. M. Srivastava, "Design and analysis of IGZO thin film transistor for AMOLED pixel circuit using double-gate tri active layer channel," *Heliyon*, vol. 5, no. 4, Apr. 2019, Art. no. e01452, doi: [10.1016/j.heliyon.2019.e01452](https://doi.org/10.1016/j.heliyon.2019.e01452).
- [5] A. Chasin, V. Volskiy, M. Libois, M. Ameys, M. Nag, M. Rockele, K. Myny, S. Steudel, S. Schols, G. A. E. Vandenbosch, W. de Raedt, J. Genoe, G. Gielen, and P. Heremans, "Integrated UHF a-IGZO energy harvester for passive RFID tags," in *IEDM Tech. Dig.*, Dec. 2013, pp. 11.3.1–11.3.4, doi: [10.1109/IEDM.2013.6724608](https://doi.org/10.1109/IEDM.2013.6724608).
- [6] A. Chasin, L. Zhang, A. Bhoolakam, M. Nag, S. Steudel, B. Govoreanu, G. Gielen, and P. Heremans, "High-performance a-IGZO thin film diode as selector for cross-point memory application," *IEEE Electron Device Lett.*, vol. 35, no. 6, pp. 642–644, Jun. 2014, doi: [10.1109/LED.2014.2314704](https://doi.org/10.1109/LED.2014.2314704).
- [7] J. Kaczmarek, J. Grochowski, E. Kaminska, A. Taube, W. Jung, and A. Piotrowska, "In-Ga-Zn-O MEFET with transparent amorphous Ru-Si-O Schottky barrier," *Phys. Status Solidi-Rapid Res. Lett.*, vol. 8, no. 7, pp. 625–628, Jul. 2014, doi: [10.1002/pssr.201409124](https://doi.org/10.1002/pssr.201409124).
- [8] J. Kaczmarek, J. Jankowska-Sliwińska, and M. A. Borysiewicz, "IGZO MEFET with enzyme-modified Schottky gate electrode for glucose sensing," *Jpn. J. Appl. Phys.*, vol. 58, no. 9, May 2019, Art. no. 090603, doi: [10.7567/1347-4065/ab1a65](https://doi.org/10.7567/1347-4065/ab1a65).
- [9] Q. Guo, F. Lu, Q. Tan, T. Zhou, J. Xiong, and W. Zhang, "Al<sub>2</sub>O<sub>3</sub>-based a-IGZO Schottky diodes for temperature sensing," *Sensors*, vol. 19, no. 2, p. 224, Jan. 2019, doi: [10.3390/s19020224](https://doi.org/10.3390/s19020224).
- [10] A. Chasin, S. Steudel, K. Myny, M. Nag, T.-H. Ke, S. Schols, J. Genoe, G. Gielen, and P. Heremans, "High-performance a-In-Ga-Zn-O Schottky diode with oxygen-treated metal contacts," *Appl. Phys. Lett.*, vol. 101, no. 11, Sep. 2012, Art. no. 113505, doi: [10.1063/1.4752009](https://doi.org/10.1063/1.4752009).
- [11] A. Chasin, M. Nag, A. Bhoolakam, K. Myny, S. Steudel, S. Schols, J. Genoe, G. Gielen, and P. Heremans, "Gigahertz operation of a-IGZO Schottky diodes," *IEEE Trans. Electron Devices*, vol. 60, no. 10, pp. 3407–3412, Oct. 2013, doi: [10.1109/TED.2013.2275250](https://doi.org/10.1109/TED.2013.2275250).
- [12] L. A. Santana, L. M. Reséndiz, A. I. Díaz, F. J. Hernandez-Cuevas, M. Aleman, and N. Hernandez-Como, "Schottky barrier diodes fabricated with metal oxides AgOx/IGZO," *Microelectronic Eng.*, vol. 220, Feb. 2020, Art. no. 111182, doi: [10.1016/j.mee.2019.111182](https://doi.org/10.1016/j.mee.2019.111182).
- [13] J. Zhang, Y. Li, B. Zhang, H. Wang, Q. Xin, and A. Song, "Flexible indium-gallium-zinc-oxide Schottky diode operating beyond 2.45 GHz," *Nature Commun.*, vol. 6, no. 1, p. 7561, Jul. 2015, doi: [10.1038/ncomms8561](https://doi.org/10.1038/ncomms8561).
- [14] S. Ho, H. Yu, and F. So, "Transparent indium-tin oxide/indium-gallium-zinc oxide Schottky diodes formed by gradient oxygen doping," *Appl. Phys. Lett.*, vol. 111, no. 21, Nov. 2017, Art. no. 212103, doi: [10.1063/1.4993430](https://doi.org/10.1063/1.4993430).
- [15] J. Zhang, Q. Xin, and A. Song, "High performance Schottky diodes based on indium-gallium-zinc-oxide," *J. Vac. Sci. Technol. A, Vac. Surf. Films*, vol. 34, no. 4, Apr. 2016, Art. no. 04C101, doi: [10.1116/1.4945102](https://doi.org/10.1116/1.4945102).
- [16] D. H. Lee, K. Nomura, T. Kamiya, and H. Hosono, "Diffusion-limited a-IGZO/Pt Schottky junction fabricated at 200 °C on a flexible substrate," *IEEE Electron Device Lett.*, vol. 32, no. 12, pp. 1695–1697, Dec. 2011, doi: [10.1109/LED.2011.2167123](https://doi.org/10.1109/LED.2011.2167123).
- [17] T.-C. Fung, C.-S. Chuang, C. Chen, K. Abe, R. Cottle, M. Townsend, H. Kumomi, and J. Kanicki, "Two-dimensional numerical simulation of radio frequency sputter amorphous In-Ga-Zn-O thin-film transistors," *J. Appl. Phys.*, vol. 106, no. 8, Oct. 2009, Art. no. 084511, doi: [10.1063/1.3234400](https://doi.org/10.1063/1.3234400).
- [18] V. Ulianova, S. Bolat, G. Torres Sevilla, I. Shorubalko, and Y. Romanyuk, "Effects of oxygen content and thermal annealing on sputtered a-IGZO Schottky diodes," in *Proc. IEEE 39th Int. Conf. Electron. Nanotechnol. (ELNANO)*, Apr. 2019, pp. 88–91, doi: [10.1109/ELNANO.2019.8783577](https://doi.org/10.1109/ELNANO.2019.8783577).
- [19] S. M. Sze and K. K. Ng, *Physics of Semiconductor Devices*, 3rd ed. New York, NY, USA: Wiley, 2007.
- [20] A. Takagi, K. Nomura, H. Ohta, H. Yanagi, T. Kamiya, M. Hirano, and H. Hosono, "Carrier transport and electronic structure in amorphous oxide semiconductor, a-InGaZnO<sub>4</sub>," *Thin Solid Films*, vol. 486, nos. 1–2, pp. 38–41, Aug. 2005, doi: [10.1016/j.tsf.2004.11.223](https://doi.org/10.1016/j.tsf.2004.11.223).

- [21] H. Qian, C. Wu, H. Lu, W. Xu, D. Zhou, F. Ren, D. Chen, R. Zhang, and Y. Zheng, "Bias stress instability involving subgap state transitions in a-IGZO Schottky barrier diodes," *J. Phys. D, Appl. Phys.*, vol. 49, no. 39, Sep. 2016, Art. no. 395104, doi: [10.1088/0022-3727/49/39/395104](https://doi.org/10.1088/0022-3727/49/39/395104).
- [22] H. Wang, X. Chen, G.-H. Xu, and K.-M. Huang, "A novel physical parameter extraction approach for Schottky diodes," *Chin. Phys. B*, vol. 24, no. 7, Jun. 2015, Art. no. 077305, doi: [10.1088/1674-1056/24/7/077305](https://doi.org/10.1088/1674-1056/24/7/077305).
- [23] J.-W. Kim, T.-J. Jung, and S.-M. Yoon, "Device characteristics of Schottky barrier diodes using In-Ga-Zn-O semiconductor thin films with different atomic ratios," *J. Alloys Compounds*, vol. 771, pp. 658–663, Jan. 2019, doi: [10.1016/j.jallcom.2018.08.289](https://doi.org/10.1016/j.jallcom.2018.08.289).
- [24] S. Kahng, "Design fundamentals and advanced techniques of RFID antennas," in *Development and Implementation of RFID Technology*, C. Turcu, Ed. London, U.K.: IntechOpen, Jan. 2009. [Online]. Available: [http://www.intechopen.com/books/development\\_and\\_implementation\\_of\\_rfid\\_technology/design\\_fundamentals\\_and\\_advanced\\_techniques\\_of\\_rfid\\_antennas](http://www.intechopen.com/books/development_and_implementation_of_rfid_technology/design_fundamentals_and_advanced_techniques_of_rfid_antennas), doi: [10.5772/6517](https://doi.org/10.5772/6517).
- [25] P. Nenzi and H. Vogt. (Jun. 1, 2011). *Ngspice User Manual, Version 23*. [Online]. Available: <https://www.iitg.ac.in/cseweb/vlab/vlsi/Experiments/ngspice23-manual.pdf>
- [26] A. Tataroğlu and Ş. Altındal, "Characterization of current-voltage (I-V) and capacitance-voltage-frequency (C-V-f) features of Al/SiO<sub>2</sub>/p-Si (MIS) Schottky diodes," *Microelectronic Eng.*, vol. 83, no. 3, pp. 582–588, Mar. 2006, doi: [10.1016/j.mee.2005.12.014](https://doi.org/10.1016/j.mee.2005.12.014).

**VERONIKA ULIANOVA** received the Ph.D. degree in solid-state electronics from the National Technical University of Ukraine "Igor Sikorsky Kyiv Polytechnic Institute", in 2016. She was a Teaching Assistant at the Faculty of Electronics, National Technical University of Ukraine "Igor Sikorsky Kyiv Polytechnic Institute". Her research interests include the synthesis of oxide semiconductor materials, including nanostructures for thin-film device applications. She was awarded a Marie Skłodowska-Curie Fellowship as part of the EU-funded EMPAPOSTDOCS-II Project from the Empa–Swiss Federal Laboratories for Materials Science and Technology, in 2018.

**FARHAN RASHEED** received the M.Sc. degree in nanoelectronic systems from the Technische Universität Dresden, Dresden, Germany, in 2016. He is currently pursuing the Ph.D. degree in process design kit development for printed electronics with the Chair of Dependable Nano Computing, Karlsruhe Institute of Technology, Karlsruhe, Germany. His current research interests include device modeling, circuit design, physical design automation, and process design kit development.

**SAMI BOLAT** (Graduate Student Member, IEEE) received the M.Sc. degree in electrical and electronics engineering from Bilkent University, Turkey, in 2014. He performs his Doctoral Research with the Laboratory for Thin Films and Photovoltaics with Empa-Swiss Federal Laboratories for Materials Science and Technology, and he is enrolled as a Ph.D. student with ETH Zürich. His research aims at demonstrating fully printed transistors with oxide materials on flexible substrates. He has authored and coauthored 18 papers in various scientific journals and conference proceedings. He received the "IEEE Electron Devices Society Ph.D. Student Fellowship", in 2019, for his academic and research-related achievements.

**GALO TORRES SEVILLA**, photograph and biography not available at the time of publication.

**YURI DIDENKO** received the Ph.D. degree in solid-state electronics from the National Technical University of Ukraine "Igor Sikorsky Kyiv Polytechnic Institute", in 2016. He is currently an Associate Professor with the Department of microelectronics, National Technical University of Ukraine "Igor Sikorsky Kyiv Polytechnic Institute". His research interests include the novel materials for microwave applications.

**XIAOWEI FENG** received the B.Sc. degree in systems engineering and automation from Tongji University, China, in 2013, and the M.Sc. degree in electrical engineering from RWTH Aachen University, Germany, in 2016. He is currently pursuing the Ph.D. degree with the Karlsruhe Institute of Technology, Germany. His research interest includes device modeling, analog design, and process design kit development in printed electronics.

**IVAN SHORUBALKO** received the Ph.D. degree in physics from Lund University, Lund, Sweden. The focus of his research was on electrical properties of quantum and ballistic nanodevices fabricated from III–V semiconductors. Then, he was a Postdoctoral Researcher in the nanophysics group at ETH Zurich, Switzerland, working on designing and manipulating electron quantum states in semiconductor nanostructures based. He joined Empa–Swiss Federal Laboratories for Materials Science and Technology Switzerland as a Scientist, in 2009, and developed to a Group Leader. His current research interests are novel nanoelectronics and nanophotonic components. Recent developments: hybrid quantum dots–graphene infrared detectors, electrical rectification effect in three-terminal graphene nano-junctions, miniaturized waveguide imaging spectrometers based on plasmonic antennas, focused He-ion beam nanostructuring technique for novel devices.

**DOMINIK BACHMANN** received the B.Sc. degree in electrical engineering from the Zurich University of Applied Sciences and the M.Sc. degree from the University of Freiburg. His professional expertise includes circuit design, general electronics, low noise electronics, high-frequency electronics, digital electronics, Arduino and low-level microprocessors, CPLD/VHDL, electrical characterization, and apprentices teaching (SVEB I).

**DMYTRO TATARCHUK** received the Ph.D. degree in solid-state electronics from the National Technical University of Ukraine, in 2001. He is an Associate Professor at the Department of microelectronics, National Technical University of Ukraine "Igor Sikorsky Kyiv Polytechnic Institute". His research interests include the microwave electronics, dielectric materials, including nanomaterials.

**MEHDI B. TAHOORI** (Senior Member, IEEE) received the B.S. degree in computer engineering from Sharif University, Tehran, Iran, in 2000, and the M.S. and Ph.D. degrees in electrical engineering from Stanford University, Stanford, CA, USA, in 2002 and 2003, respectively.

He is currently a Professor with the Chair of Dependable Nano Computing, Karlsruhe Institute of Technology, Karlsruhe, Germany. He has authored over 250 conference papers and journal articles.

**JASMIN AGHASSI-HAGMANN** (Member, IEEE) received the M.Sc. degree in physics from RWTH Aachen University, Aachen, Germany, and the Ph.D. degree from the Karlsruhe Institute of Technology (KIT), Karlsruhe, Germany.

She joined Infineon Technologies AG, Neubiberg, Germany, in 2007, and Intel Mobile Communications GmbH, Munich, Germany, in 2011. She joined the KIT as a Group Leader, in 2012.

**YAROSLAV E. ROMANYUK** received the Ph.D. degree from the Swiss Federal Institute of Technology, Lausanne, in 2005. After his postdoctoral stay at the University of California at Berkeley, Berkeley, he joined Empa–Swiss Federal Laboratories for Materials Science and Technology as a Group Leader of the Laboratory for Thin Films and Photovoltaics, in 2008. His research interests include novel materials for thin-film solar cells, solid-state batteries, and oxide electronics fabricated with vacuum and printing methods. He holds several patents and has coauthored more than 110 research articles.

• • •